

## Supporting Information

### Lanthanide-binding peptides for NMR measurements of residual dipolar couplings and paramagnetic effects from multiple angles

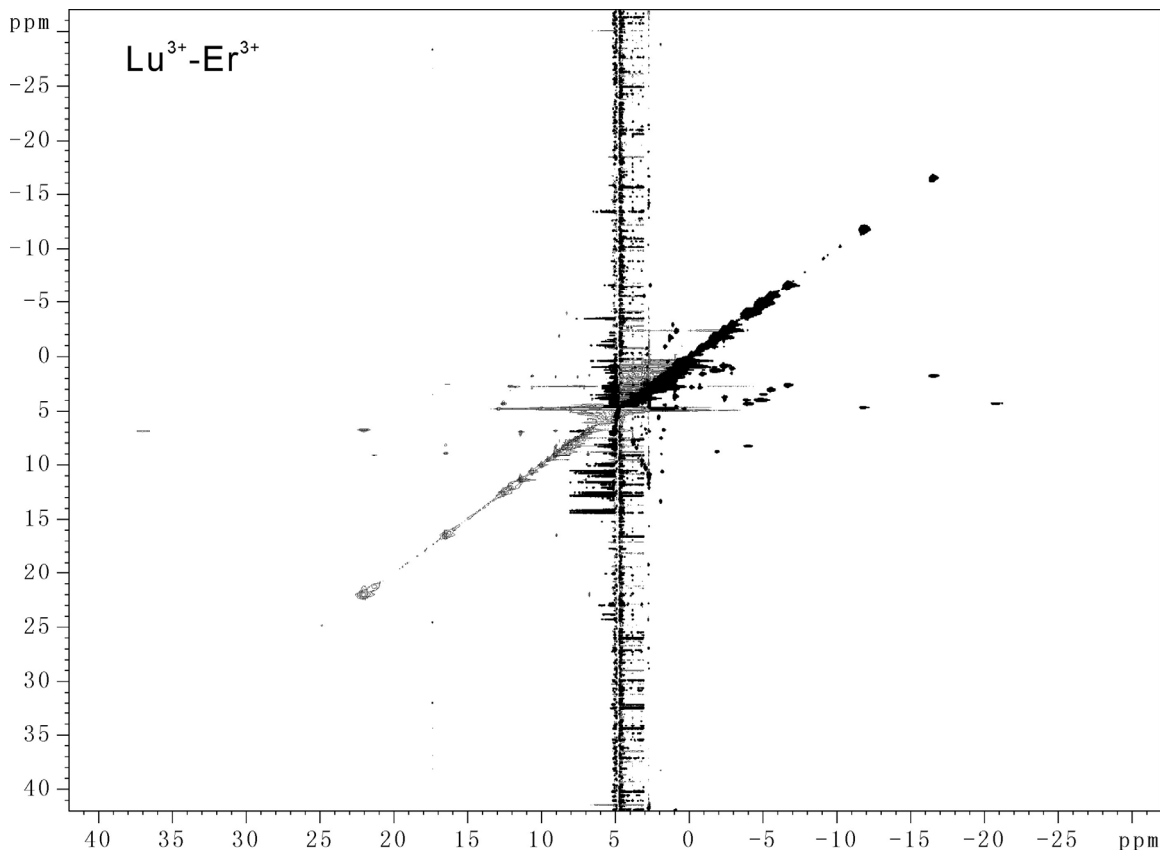
Xun-Cheng Su, Kerry McAndrew, Thomas Huber, Gottfried Otting

**Table S1**  $^1\text{H}$  chemical shifts of the LBT4-Lu $^{3+}$  complex<sup>a</sup>

residue	$\text{H}^{\text{N}}$	$\text{H}^{\alpha}$	$\text{H}^{\beta}$	others			
<b>Cys 0</b>							
Tyr 1		4.70	2.69 1.76	$\text{C}^{\text{d}}\text{H}_2$	6.92	$\text{C}^{\text{e}}\text{H}_2$	6.76
Val 2	8.90 (8.90)	4.31	2.04	$\text{C}^{\gamma}\text{H}_3$	0.93 0.91		
Asp 3	9.10 (9.07)	4.87	2.81 2.24				
Thr 4	8.05 (7.93)	3.96	4.30	$\text{C}^{\gamma}\text{H}_3$	1.30		
Asn 5	8.37 (8.25)	4.85	3.34 2.92	$\text{N}^{\delta}\text{H}_2$	8.35 6.95		
Asn 6	8.01 (7.88)	4.31	3.05 2.58				
Asp 7	8.10 (7.93)	4.65	3.02 2.37				
Gly 8	9.56 (9.45)	4.04 3.49					
Ala 9	7.77 (7.61)	4.48	1.20				
Tyr 10	9.16 (9.10)	5.58	2.71 2.52	$\text{C}^{\delta}\text{H}_2$	6.89	$\text{C}^{\text{e}}\text{H}_2$	6.73
Glu 11	8.54 (8.41)	4.67	2.33 1.81	$\text{C}^{\gamma}\text{H}_2$	2.39 1.92		
Gly 12	8.78 (8.72)	3.96 3.70					
Asp 13	9.01 (9.00)	4.58	2.85 2.80				
Glu 14	8.26 (8.14)	4.42	2.57 2.27	$\text{C}^{\gamma}\text{H}_2$	2.89 2.82		
Leu 15	7.06 (6.91)	4.02	1.59 1.38	$\text{C}^{\gamma}\text{H}$	1.06	$\text{C}^{\delta}\text{H}_3$	0.78 0.27

<sup>a</sup> In ppm at 25 °C.  $\text{H}^{\text{N}}$  chemical shifts at 10 °C are shown in brackets.

**Figure S1.** EXSY spectra of complexes of LBT4 with mixtures of Lu<sup>3+</sup> and paramagnetic lanthanide ions at 25 °C. The peptide concentration was 1.5 mM in the presence of 4 mM glycine, 4 mM DTT, and 20 mM MES at pH 6.5. The mixing time was 5 ms. (a) [LBT4] : [Lu<sup>3+</sup>] : [Er<sup>3+</sup>] = 1 : 0.5 : 0.6; (b) [LBT4] : [Lu<sup>3+</sup>] : [Tm<sup>3+</sup>] = 1 : 0.5 : 0.6; (c) [LBT4] : [Lu<sup>3+</sup>] : [Yb<sup>3+</sup>] = 1 : 0.5 : 0.6.



(a)

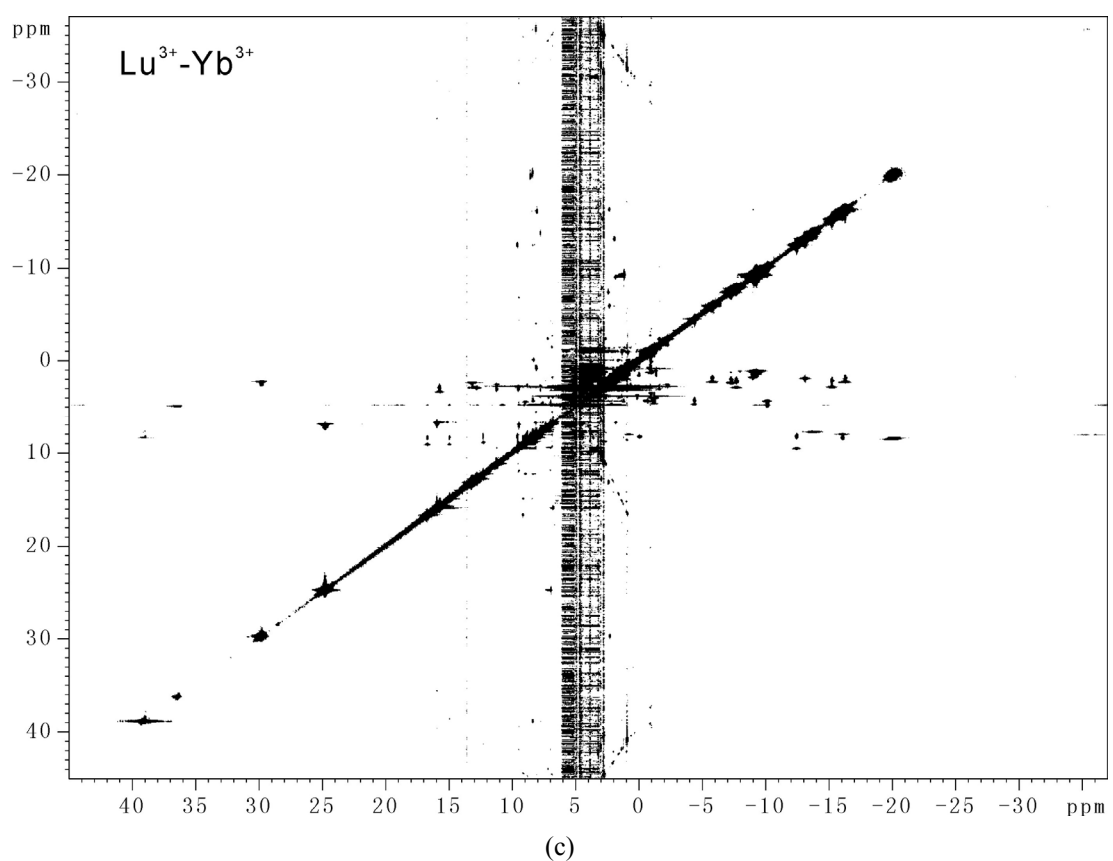
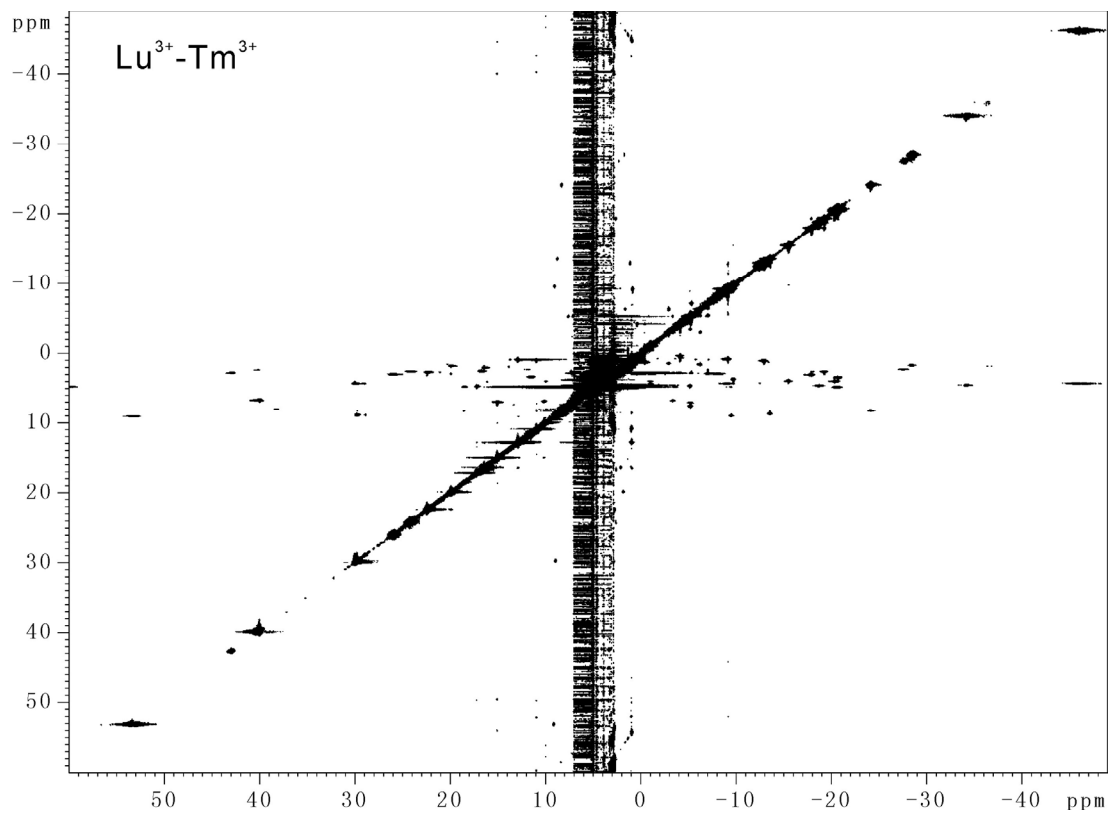


**Table S2.** Chemical shifts of backbone amide protons of LBT4 in complexes with Er<sup>3+</sup>, Yb<sup>3+</sup>, or Tm<sup>3+</sup> <sup>a</sup>

residue	25 °C			10 °C	
	Er <sup>3+</sup>	Yb <sup>3+</sup>	Tm <sup>3+</sup>	Yb <sup>3+</sup>	Tm <sup>3+</sup>
Val 2	16.48	12.24	29.72	12.79	33.41
Asp 3	21.35	14.91	53.18	15.84	61.26
Thr 4		0.74	38.30	0.50	
Asn 5		-20.32			
Asn 6		-16.14		-18.91	
Asp 7		-35.80			
Gly 8		-12.51		-14.28	
Ala 9		2.70			
Tyr 10		16.66		16.37	
Glu 11		-19.92		-22.56	
Gly 12	-1.90	2.54	-13.64	1.99	-16.34
Asp 13	1.84				-12.11
Glu 14	-3.96	-0.09	-24.21	-0.87	-28.88
Leu 15	2.87	4.39	-5.31	3.58	-7.30

<sup>a</sup> Chemical shifts in ppm.

**Table S3.** PCS of backbone amide protons of ArgN-LBT-Tm<sup>3+</sup> complexes at 10 °C <sup>a</sup>

residue	ArgN-LBT2	ArgN-LBT3	ArgN-LBT4	ArgN-LBT5
Leu 10	0.29	-0.20	0.28	0.35
Phe 11		-0.23	0.34	
Lys 12	0.44		0.41	0.52
Ala 13	0.55	-0.23	0.46	0.61
Phe 14	0.60	-0.30	0.53	0.73
Lys 15	0.79	-0.41	0.74	0.97
Ala 16	0.87	-0.36	0.81	
Leu 17		-0.36	0.81	
Leu 18	1.17	-0.58	1.01	
Lys 19	1.41			
Ser 24		-0.21	0.51	
Ser 25	0.66			
Gln 26		-0.37		0.37
Gly 27	0.29	-0.26	0.21	0.33
Glu 28	0.42	-0.27	0.29	0.46
Ala 29	0.50	-0.29	0.38	0.63
Phe 30		-0.25	0.31	0.49
Ala 31	0.36	-0.14	0.32	0.40
Ala 32	0.41	-0.19	0.34	
Leu 33	0.41	-0.19	0.36	
Gln 34	0.32	-0.15	0.26	0.42
Glu 35	0.32	-0.12	0.28	
Gln 36	0.33	-0.12	0.24	0.42
Gly 37	0.28	-0.09	0.24	0.37
Phe 38	0.28	-0.11	0.19	0.36
Asp 39	0.27	-0.14	0.15	0.26
Asn 40		-0.12	0.18	0.22
Ile 41		-0.13	0.17	
Asn 42	0.22	-0.19	0.11	0.26
Gln 43	0.21			0.22
Ser 44	0.18	-0.19	0.14	0.18
Lys 45	0.23	-0.21	0.19	0.22
Val 46	0.33	-0.26	0.20	
Ser 47	0.35	-0.30	0.15	0.30
Arg 48	0.25	-0.31	0.24	0.24
Met 49	0.35	-0.38	0.26	0.36
Leu 50	0.57	-0.53	0.25	
Thr 51	0.48	-0.57	0.24	0.33
Lys 52	0.43	-0.55	0.50	
Phe 53	0.77	-0.74	0.52	
Gly 54	0.87	-0.98	0.35	0.43
Ala 55	1.29	-1.21		
Val 56	2.68			
Lys 62	1.05			
Met 63	0.97			
Met 65	0.74			
Val 66				1.27
Tyr 67	1.38			
Cys 68	2.55			
Leu 69	2.99			

<sup>a</sup> PCS values in ppm.

**Table S4.** RDCs of backbone amides measured for ArgN-LBT complexes with Tm<sup>3+</sup> <sup>a</sup>

residue	ArgN-LBT2	ArgN-LBT3	ArgN-LBT4	ArgN-LBT5
Leu 10	-2.8	-6.8	-5.1	-0.7
Phe 11		-5.6	-6.2	
Lys 12	8.4	-9.6	1.7	6.7
Ala 13	0.8	-9.2	-1.5	4.2
Phe 14	-4.7	-4.6	-3.3	-1.7
Lys 15	-0.9	-5.0	-3.4	-2.7
Ala 16	8.4	-10.9	1.9	
Leu 17			-2.3	
Leu 18	-7.7	-4.0		
Ser 24	13.6			
Gly 27	2.2		2.8	4.8
Glu 28	22.6	-0.7	16.0	21.4
Ala 29	10.9	6.6	10.0	9.8
Phe 30		4.1		6.0
Ala 31	9.4		2.8	
Leu 33	8.7	5.2		
Gln 34	5.8	2.8	1.9	4.3
Glu 35	17.8	-5.2	12.1	17.8
Gln 36		4.5		10.4
Phe 38	-1.8	-8.6		2.6
Asp 39		0.3		-6.4
Asn 40	-2.3	0.6		-4.8
Asn 42		-1.9		-6.6
Gln 43				-3.2
Ser 44	7.4	-7.8	7.8	8.2
Lys 45	13.5	-4.5	12.6	7.9
Val 46	-2.5		-0.3	
Ser 47	3.6	-3.7	4.2	2.5
Arg 48	16.5	-7.5	13.7	13.3
Met 49	6.8	-2.6	11.0	
Leu 50	-3.4			-4.0
Thr 51	3.2	-5.4	4.5	4.1
Lys 52	12.5	-4.5		
Phe 53	-2.2	-1.0	0.3	-6.2
Gly 54	-8.8	0.1		-2.0
Met 65	-9.3			

<sup>a</sup> RDCs measured in Hz as the splitting observed for the Lu<sup>3+</sup> complex minus the splitting observed for the Tm<sup>3+</sup> complex at 10 °C and a <sup>1</sup>H NMR frequency of 800 MHz.

**Table S5.**  $\Delta\chi$  tensors of ArgN-LBT-Tm<sup>3+</sup> complexes obtained by fitting the PCS of the amide protons of ArgN (Table S3) with the solution structure of ArgN <sup>a</sup>

construct	$\chi_{ax}$	$\chi_{rh}$	$\chi_{xx}$	$\chi_{yy}$	$\chi_{zz}$	tensor axis	coordinates of tensor axes		
ArgN-LBT2	23.1	14.4	-0.5	-14.9	15.4	x	-0.618	0.523	-0.587
						y	-0.173	0.638	0.751
						z	0.767	0.565	-0.304
ArgN-LBT3	-13.3	-2.7	3.1	5.8 <sup>b</sup>	-8.9 <sup>b</sup>	x	-0.235	0.584	-0.777
						y	-0.728	0.424	0.538
						z	0.644	0.693	0.326
ArgN-LBT4	22.8	13.6	-0.8	-14.4	15.2	x	-0.670	0.509	-0.540
						y	-0.049	0.696	0.717
						z	0.740	0.507	-0.442
ArgN-LBT5	22.0	5.9	-4.4	-10.3	14.7	x	-0.336	-0.239	-0.911
						y	-0.658	0.751	0.046
						z	0.674	0.615	-0.410

<sup>a</sup> The tensor parameters are in units of 10<sup>-32</sup> m<sup>3</sup>. The axes refer to conformer 8 of the NMR structure of ArgN (PDB code 1AOY).

<sup>b</sup> The y and z axes of this tensor are swapped compared to the alignment tensor (see Figures 4 and S2) to satisfy the condition  $|\chi_{zz}| > |\chi_{yy}| > |\chi_{xx}|$ .

**Figure S2.** Stereoview of a ribbon representation of ArgN illustrating the  $\Delta\chi$  tensor axes of different ArgN-LBT-Tm<sup>3+</sup> complexes. The tensor axes are centered at the positions of the metal ions as determined by best fitting. The x, y, and z-axes (as defined in Table S5) are shown in cyan, blue, and red, respectively. The numbers refer to the LBT numbering in Table 1.

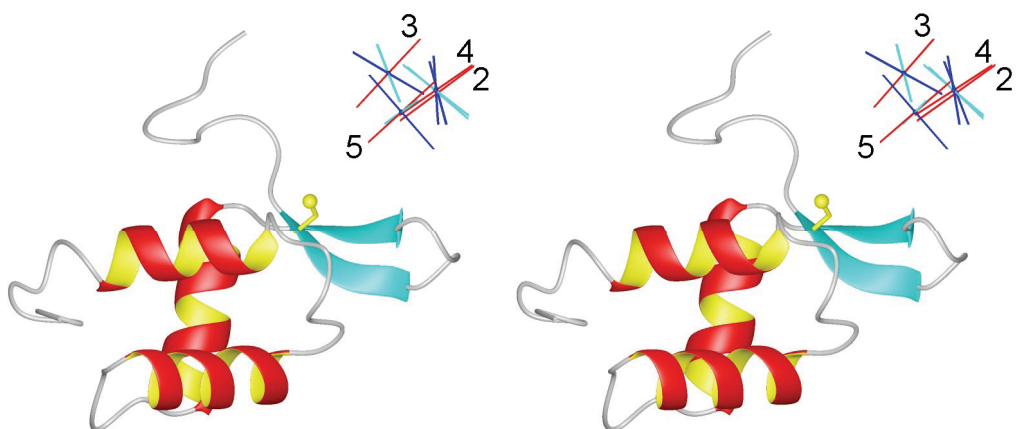


**Figure S3.** Isosurfaces of the PCS of  $\text{Tm}^{3+}$  complexes of (a) ArgN-LBT2 and (b) ArgN-LBT3. The isosurfaces were calculated for PCS of  $\pm 3$ ,  $\pm 1$  and  $\pm 0.3$  ppm. Blue and red surfaces identify positive and negative PCS, respectively.

